# Enhancing Sulfur Oxidation Reaction by Overcoming Redox Barriers with $FeSe_2$@C for Lithium-Sulfur Batteries

Pengkun Zou[a,&], Yushuang Lin[a,&], Long Li[a,&], Jiaxin Wang[a], Yu Chao[a], Borong Li[a], Hongyun Ma[b,*], Zheyuan Liu[a], Yan Yu[a,*], Chengkai Yang[a,*]

[a] Key Laboratory of Advanced Materials Technologies, International (HongKong Macao and Taiwan) Joint Laboratory on Advanced Materials Technologies, College of Materials Science and Engineering, Fuzhou University, Fuzhou, Fujian, 350108, China

[b] School of Materials and Energy, Lanzhou University, Lanzhou 730000, P. R. China.

[&] Authors contributed equally to this work

* Corresponding mails: chengkai_yang@fzu.edu.cn (C.K. Yang), yuyan@fzu.edu.cn (Y. Yu), mhy@lzu.edu.cn (H.Y. Ma).

# 1 Experimental section

## 1.1 Synthesis scheme of $FeSe_2$@C and C

Preparation of $FeSe_2$ Rod-like Nanoflower Precursor: Firstly, dissolve 6 mmol of $(NH_4)_2$ Fe $(SO_4)_2 \cdot 6H_2O$ in 40 mL of deionized water to form a homogeneous solution. Next, using a pipette, transfer 20 ml of hydrazine hydrate (85%) to a beaker, add a stirring bar, and weigh 12 mmol of selenium powder. Slowly add the hydrazine hydrate solution to the beaker containing the selenium powder while stirring, and continue stirring for 30 minutes until the solution turns deep reddish-brown. Then, slowly drip the selenium powder solution into the previous solution and continue stirring for another 30 minutes. Transfer the mixture into a polytetrafluoroethylene inner container and place it in a stainless-steel reaction vessel. Set the program temperature to 180°C and maintain it for 8 hours, followed by natural cooling to room temperature. After reaching room temperature, collect the black precipitate, wash it with deionized water, and centrifuge it three times. Subsequently, vacuum dry the collected black powder sample, denoted as $FeSe_2$.

Preparation of $FeSe_2$@C: 1000 mg of dopamine hydrochloride was weighed and dissolved in 500 mL of 0.01 mol/L Tris-HCl buffer (pH=8.5) with stirring for 10 minutes, resulting in a reddish-brown solution. The self-polymerization temperature was maintained at 40°C, and the self-polymerization process continued for 12 hours at a stirring speed of 1500 rpm. Then, an appropriate amount (125 mg) of the previously prepared $FeSe_2$ material was added, and the resulting mixture was collected by centrifugation. The collected product was washed several times with water and ethanol and subsequently dried using a vacuum drying oven for later use. The collected black product was placed in a tube furnace under nitrogen protection and heated at a rate of 2°C/min until reaching 500°C, and then kept at this temperature for 2 hours to obtain $FeSe_2$ rod-like nanoflower coated with porous carbon ($FeSe_2$@C).

Preparation of C: Commercial conductive carbon black was used as the carbon material, serving as the control group for comparison.

## 1.2 Preparation of the electrolyte and $Li_2S_6$ catholyte

The electrolyte was made of (1 M lithium bis(trifluoromethanesulfonyl)imide and 0.2 M lithium nitrate in the mixed solvent of 1,3-dioxolane and 1,2-dimethoxymethane with volume ratio of 1:1). The $Li_2S_6$ catholyte (1M) was prepared by reacting the sublimed sulfur with $Li_2S$ in stoichiometric proportion in the blank electrolyte. The mixture was vigorously stirred at 50 ℃ in an argon-filled glove box overnight to produce a brownish-red $Li_2S_6$ catholyte solution.

**1.3 Synthesis of the sulfur-containing cathodes**

Sublimed sulfur and $FeSe_2$ (or conductive carbon black) materials were weighed in a weight ratio of 8:2 and placed into a mortar. The mixture was then ground for 15-30 minutes to ensure a homogeneous blend. Next, the mixed powder was transferred into a reaction vessel filled with argon gas and placed in a muffle furnace. The mixture was kept at 155 ℃ for 12 hours and subsequently allowed to cool naturally to room temperature. The resulting material, $FeSe_2$@C/S, was obtained and used as the positive electrode material.

**1.4 Cell assembly and electrochemical measurements**

The cathode fabrication involved the preparation of a slurry containing 80 wt% of active materials ($FeSe_2$@C/S), Super P (10 wt%), and PVDF (10 wt%), which was then pasted onto a aluminum foil collector plate. Subsequently, the assembled batteries were created by cutting the dried slurry into circular pellets, the sulfur loading is approximately 1 mg $cm^{-2}$. For the battery assembly, commercial separator Celgard 2400 sheet (16 mm) was employed, along with a lithium plate (12 mm) acting as the anode. These components were utilized to form 2032 cells, and the entire assembly process took place in a glove box filled with argon gas. Inject electrolyte according to Electrolyte/Sulfur =10 μL/mg. For the high sulfur loading cells, the sulfur loading was varied between 3.0 and 4.2 mg $cm^{-2}$, the cathode slurry is coated onto carbon cloth. After a static period of 12 hours, a galvanostatic charge-discharge test was conducted within a voltage range of 1.7 to 2.8 V. It is important to note that all electrochemical tests were conducted at ambient temperatures, approximately 25 °C. The barrier value is governed by the reciprocal of the charge transfer resistance ($R_{CT}$) and the reciprocal of the absolute temperature ($R_{CT} = RT/nFi_0$, where R is the universal gas constant, T is

the absolute temperature in Kelvin, n is the number of transferring electrons, F is the Faraday constant, $i_0$ is the exchange current density), following the Arrhenius relationship $i_0 \propto k = A \times e^{-Ea/RT}$. The charge transfer resistance at different temperatures was probed using the CHI760E electrochemical workstation. Electrochemical impedance spectroscopy (EIS) tests were conducted at various temperatures with 0.1 V intervals, a frequency range of 0.01-$10^5$ Hz, and an amplitude of 5 mV. Discharge to 1.7 V was initially performed at 0.05 C current density, followed by charging to the desired potential at 0.05 C and maintaining it at that potential (potentiostatic mode) until the current remained constant. Error bars were determined through measurements on three independent cells, representing standard deviations. The assembled symmetrical cells were subjected to cyclic voltammetry (CV) testing within the potential range of -0.8 V to 0.8 V at a scan rate of 50 mV $s^{-1}$. Furthermore, the entire cell system was also subjected to cyclic voltammetry within a wider potential range of 1.7 V to 2.8 V at a lower scan rate of 0.1 mV $s^{-1}$.

**1.5 Characterizations**

The morphology of the catalyst material and electrode was obtained using scanning electron microscopy (SU8010) and transmission electron microscopy (FEI TECNAI G2 F20). X-ray photoelectron spectroscopy (XPS) analysis (EXCALAB 250) was performed to determine the surface chemical composition and elemental valence. In situ Raman spectroscopy was carried out using the Lab RAM HR800 Raman spectrometer. Additionally, thermal gravimetric analysis (TGA) was performed in a nitrogen environment from room temperature to 600 °C, with a heating rate of 10 °C/min, to calculate the sulfur content in the $FeSe_2$@C/S composite material.

**1.6 Computational methods**

All calculations were carried out by using Vienna ab initio simulation package (VASP), and the Perdew-Burke-Ernzerhof (PBE) under the generalized gradient approximation (GGA) was chose to deal with the electron exchange correlation interaction.[1-5] We use it to construct a 3 x 3 x 3 graphene sheet model with vacuum layerof 15 A. Then $FeSe_2$ structure is simulated on this base model. The conjugate-

gradient algorithm was used to optimize geometry. All the atoms are allowed to fully relax during the structural optimization process. The energy convergence standard of the system was set to $10^{-6}$ eV, and the force on each atom was less than -0.02 eV/Å. A $1\times1\times1$ k-point mesh was used for the Brillouin zone sampling. The cutoff energy of plane-wave basis set was 500 eV.

## 2. Supplementary Figures

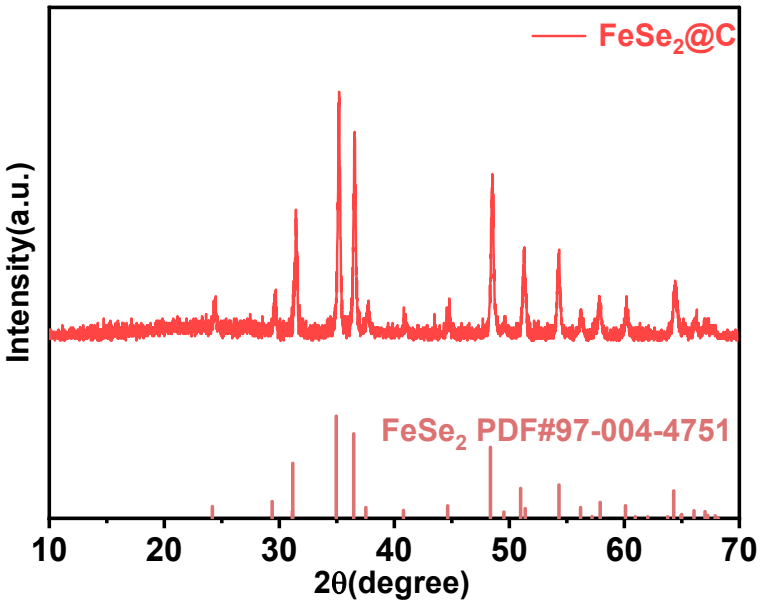


**Fig. S1.** XRD patterns of $FeSe_2$@C.

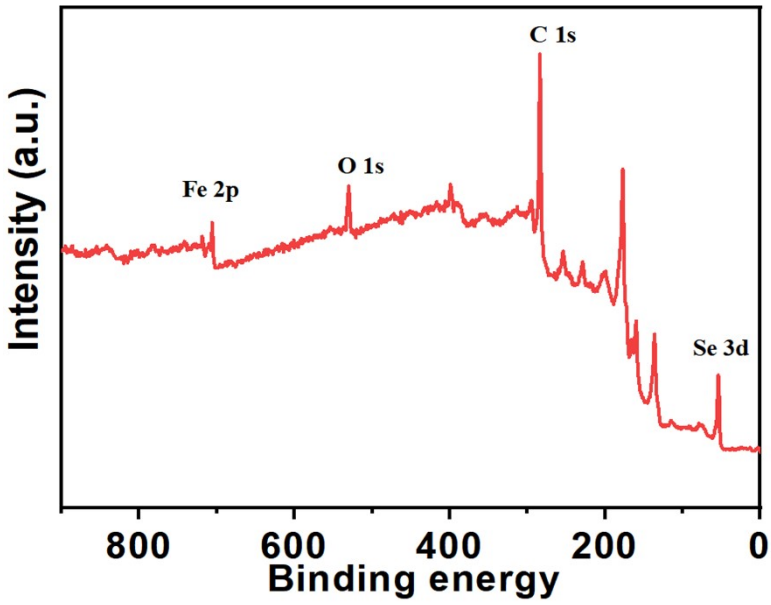


**Fig. S2.** XPS full spectrum of $FeSe_2$@C

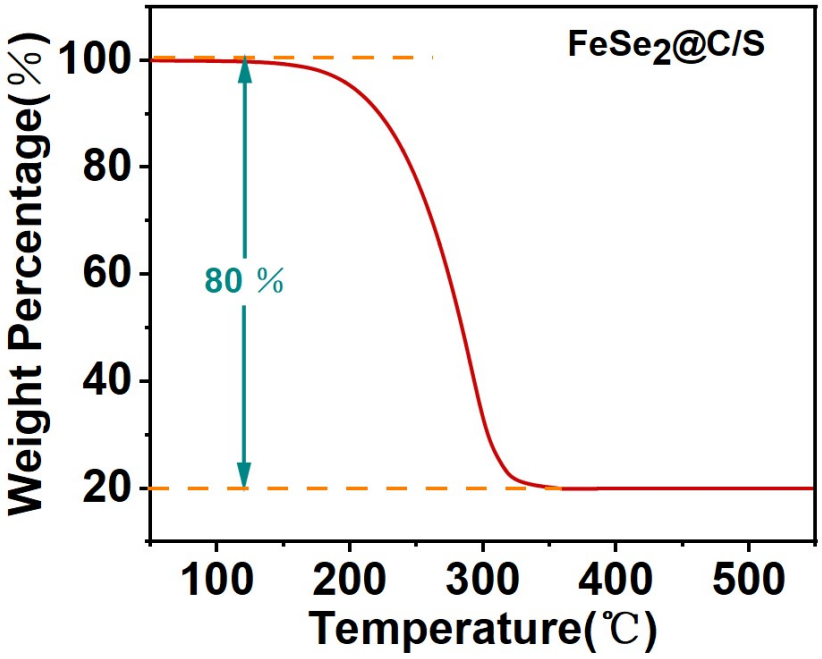


**Fig. S3.**TGA curves of sulfur and $FeSe_2$@C/S cathode

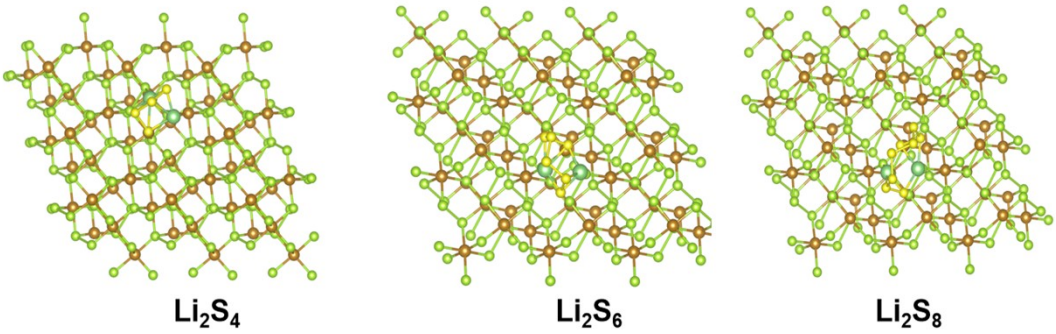


**Fig. S4.** Top-View adsorption configurations of $Li_2S_4$, $Li_2S_6$, and $Li_2S_8$ on $FeSe_2$.

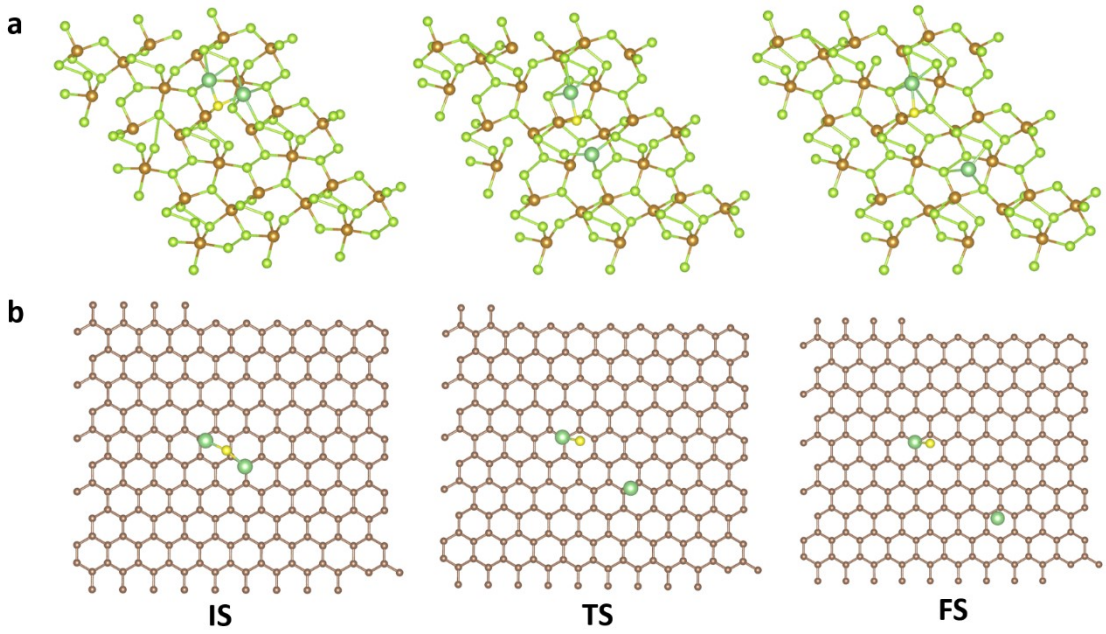


**Fig.S5** (a) Structural illustration of the $Li_2S$ decomposition process catalyzed by $FeSe_2$@C.

(b) Structural illustration of the $Li_2S$ decomposition process catalyzed by C.

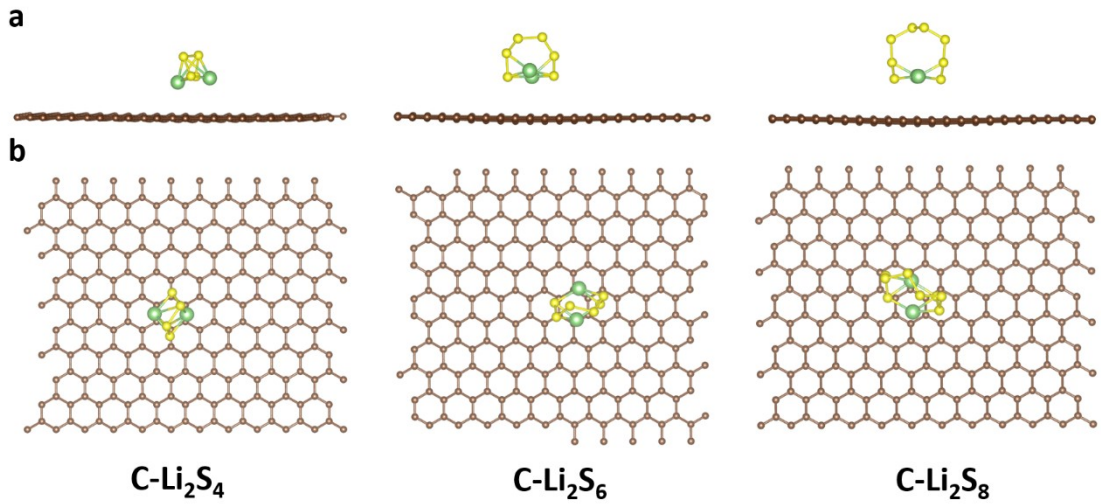


**Fig. S6.** Front view (a) and Top-View (b) adsorption configurations of $Li_2S_4$, $Li_2S_6$, and $Li_2S_8$ on $FeSe_2$

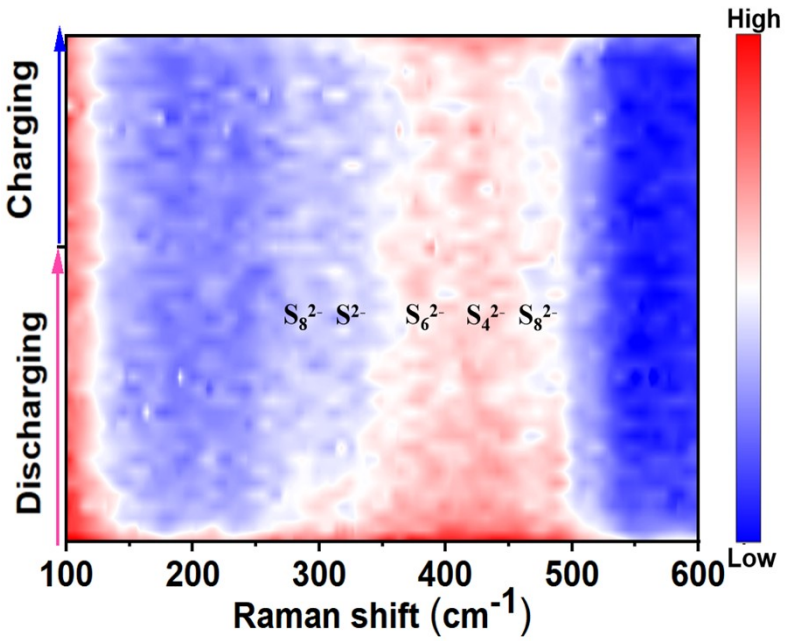


**Fig. S7** In situ Raman contour map of the C/S cathode.

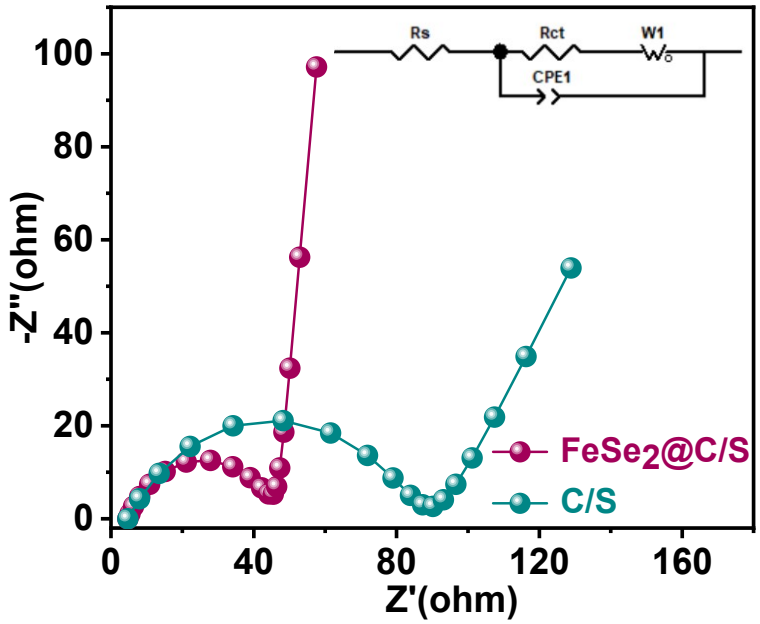


**Fig. S8** Fitted electrochemical impedance spectroscopy (EIS) diagrams.

The EIS data were fitted to an equivalent circuit model,[6] which differentiates between the ohmic resistance (Rs) associated with the internal connections of the battery components and the charge transfer resistance (Rct). The charge transfer resistance (Rct) of the polysulfides at the cathode is often utilized to characterize the kinetics of the sulfur conversion reaction. The diameter of the semicircle in the high-frequency region is typically proportional to the charge transfer resistance (Rct) associated with the conversion of polysulfides, corresponding to the charge transfer process. The results indicate that the $FeSe_2$@C electrode exhibits a charge transfer resistance (Rct) of 40 Ω, whereas the carbon (C) electrode shows an Rct of 85 Ω. The lower charge transfer resistance (Rct) of the $FeSe_2$@C electrode suggests that it can facilitate faster electron/ion transfer and possesses a higher interfacial charge conductivity. Additionally, the straight line in the low-frequency region corresponds to the diffusion process. The $FeSe_2$@C has a steeper slope compared to the carbon (C), indicating that $FeSe_2$@C possesses faster diffusion kinetics, which accelerates the ion diffusion and transport, thereby enhancing the redox reaction kinetics for the interconversion of sulfur species.

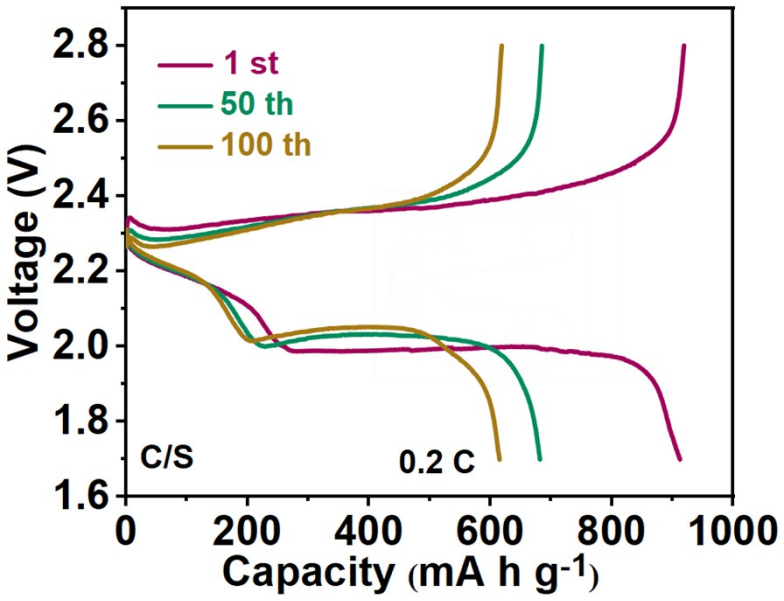


**Fig. S9** Charge-discharge curves at different cycles of C/S cathode.

1. Y. Xiao, X. Wang, K. Yang, J. Wu, Y. Chao, C. Xi, M. Li, Q. Zhang, Z. Liu and L. Li, *Energy Storage Materials*, 2023, **55**, 773-781.
2. M. Li, C. Xi, X. Wang, L. Li, Y. Xiao, Y. Chao, X. Zheng, Z. Liu, Y. Yu and C. Yang, *Small*, 2023, 2301569.
3. K. Yang, L. Li, Y. Xiao, Q. Zhang, C. Xi, B. Li, Y. Yu and C. Yang, *Chinese Chemical Letters*, 2024, **35**, 108451.
4. X. Cui, Z. Xu, C. Xi, H. Zhang, Y. Xiao, L. Li, G. Xu, X. Lyu, Q. Lin and Y. Yu, *Journal of Solid State Electrochemistry*, 2023, 1-9.
5. C. Yang, R. Shao, Q. Wang, T. Zhou, J. Lu, N. Jiang, P. Gao, W. Liu, Y. Yu and H. Zhou, *Energy Storage Materials*, 2021, **35**, 62-69.
6. X. Yu, W. Chen, J. Cai, X. Lu and Z. Sun, *Journal of Colloid and Interface Science*, 2022, **610**, 407-417.